Jurnal Teknologi

Full Paper

EFFECTS OF CROSSWINDS ON THE FLOW STRUCTURE AROUND A NEXT-GENERATION HIGH-SPEED TRAIN EXITING A TUNNEL

Mohammad Arafat*, Sakthiraaj Rajendran, Izuan Amin Ishak, Muhammad Al, Ain Mat Zin

Department of Mechanical Engineering Technology, Universiti Tun Hussein Onn Malaysia, Bandar Universiti Pagoh, Johor-84600, Malaysia

Article history
Received
29 May 2023
Received in revised form
27 April 2024
Accepted
27 April 2024
Published Online
17 October 2024

*Corresponding author
hn220016@student.uthm.edu.my

Graphical abstract

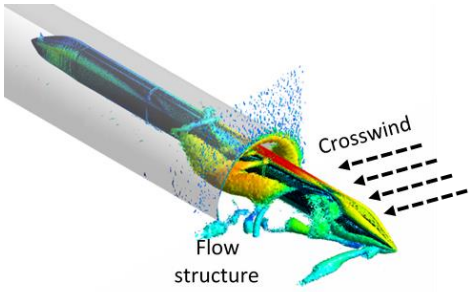

Abstract

This study investigates the effect of crosswind on the aerodynamic behavior of the Next-Generation High-Speed Train (NG-HST) model when exiting a tunnel. Utilizing a 1/25th scale model, three distinct train exit positions and four crosswind yaw angles (15°, 30°, 45°, and 60°) were considered. Computational Fluid Dynamics (CFD) simulation with the k-ε turbulence model was used to simulate the flow structure around the train at the crosswind velocity of 25 m/s. A mesh independence study was performed to ensure that the results were not influenced by mesh sizing. Furthermore, existing wind tunnel experiment data was used to validate the mesh setup. The results showed that the crosswind angle had a significant effect on the aerodynamic flow behavior of the train as it exited the tunnel. The airflow pattern on the train surface exhibited significant changes, and variations in pressure distribution were observed on both the leeward and windward sides of the train. Moreover, the cars outside the tunnel experienced greater pressure than the cars inside the tunnel. As the last car of the train emerged from the tunnel, the strong crosswind altered the vortex structure, particularly around the head car, emphasizing its critical role in ensuring safe train operation. The results can be used to improve the design of wind barriers and other infrastructure along the railway tracks to improve the operational stability and safety of high-speed trains.

Keywords: Aerodynamics, computational fluid dynamics (CFD), crosswinds, infrastructure, tunnel exit

Abstrak

Kajian ini menyiasat kesan angin lintang ke atas tingkah laku aerodinamik Kereta Api Kelajuan Tinggi Generasi Seterusnya (NG-HST) apabila keluar dari terowong. Menggunakan model skala 1/25, tiga kedudukan keluar kereta api yang berbeza dan empat sudut *yaw* lintang (15°, 30°, 45° dan 60°) telah dipertimbangkan. Simulasi *Computational Fluid Dynamics (CFD)* dengan model pergolakan k-ε digunakan untuk mensimulasikan struktur aliran di sekeliling kereta api dengan halaju angin lintang 25 m/s. Kajian kebebasan mesh telah dilakukan untuk memastikan keputusan tidak dipengaruhi oleh saiz mesh. Tambahan pula, data percubaan terowong angin sedia ada telah digunakan untuk mengesahkan persediaan mesh. Keputusan menunjukkan sudut angin lintang mempunyai kesan yang ketara terhadap tingkah laku aerodinamik kereta api semasa ia keluar dari terowong. Corak aliran udara

pada permukaan kereta api menunjukkan perubahan yang ketara, dan variasi dalam pengagihan tekanan diperhatikan pada kedua-dua bahagian bawah dan arah angin kereta api. Selain itu, kereta di luar terowong mengalami tekanan yang lebih besar daripada kereta di dalam terowong. Apabila kereta api terakhir keluar dari terowong, angin bertiup kencang telah mengubah struktur pusaran, terutamanya di sekeliling kereta utama, menekankan peranan pentingnya dalam memastikan operasi kereta api selamat. Hasilnya boleh digunakan untuk menambah baik reka bentuk penghadang angin dan infrastruktur lain di sepanjang landasan kereta api untuk meningkatkan kestabilan operasi dan keselamatan kereta api berkelajuan tinggi.

Kata kunci: Aerodinamik, dinamik bendalir pengiraan (*CFD*), angin lintang, infrastruktur, jalan keluar terowong

1.0 INTRODUCTION

The operational stability and safety of high-speed trains (HST) are major concerns for the railway industry, especially because of sudden changes in weather conditions, especially natural wind, which can lead to derailment and overturning [1]. Over the last twenty years, the development of HST has led to the construction of various types of infrastructure along the railway tracks, including bridges, tunnels, embankments, and wind barriers. For instance, railway tunnels are built for overcoming challenging terrains, improving travel time by creating shorter and more direct routes for trains [2]. When trains enter or exit a tunnel, sudden changes in wind loads and infrastructural conditions can affect the HST's operational performance.

The development of faster and lightweight structural designs for the next-generation high-speed train (NG-HST) increases concerns regarding the adverse effects of strong crosswinds on the aerodynamic performance of the train. The combined effect of a strong crosswind and fast operating speed creates unsafe events and may raise the chance of derailment. When the train's operating speed rises above 200 km/h with a crosswind speed greater than 30 m/s, the railway vehicle is likely to derail or overturn [3]. Many studies of the impacts of strong crosswinds on the aerodynamic performance of HSTs have received significant attention from researchers in various train operational conditions in the past two decades; such as flat ground [4–7] embankment [8, 9], wind barrier [10, 11], bridge [12, 13] etc,.

There has been very little research into the effects of crosswind on the aerodynamic performance of HST when a train passes through a tunnel. Previous research has shown that crosswinds have a significant impact on HST when passing different types of infrastructure when compared to flat ground and open air conditions [11, 14]. Wang *et al.,* [15] conducted a study to investigate the flow behaviour when trains exit a tunnel with a constant crosswind speed of 30 m/s. They have shown that there are transient changes in aerodynamic performance when trains exit tunnel and entered into open air zone. Moreover, transient changes in pressure distribution on the train surface were observed specifically on the leeward and windward sides. The aerodynamic effects induced by high-speed trains in tunnels can lead to pressure changes, affecting the fatigue life of train bodies and passenger comfort [16]. When crosswinds affect the train from different angles, the aerodynamic flow behavior is still unknown. As a result, it is crucial to investigate how a train performs in high crosswinds when exiting a tunnel.

Currently, there are three different methods available to study the impact of the strong crosswinds on the rail vehicles, namely, a full-scale experiment, a model-scale test, and a computational fluid dynamics (CFD) simulation. A full-scale experiment can provide accurate results that can be obtained from a real-life situation. However, it is more expensive and time-consuming. Additionally, because it is difficult to control external parameters, it is rarely used for crosswind-related studies. Aside from full-scale testing, model-scale or wind tunnel testing is much more cost-effective. Nowadays, with advancements in computational power, most of the crosswind-related studies are conducted using the CFD simulation method.

This study aims to investigate the effect of crosswind on the flow structure around HST when exiting a tunnel. For the crosswinds, four yaw angles ranging from 15° to 60° are considered. This study mainly focused on the vorticity formed around the train at different crosswind angles and train exiting positions.

2.0 METHODOLOGY

2.1 Geometry

The entire model used in this study, including the train and tunnel, was 1/25th scale. This scale model train was used by previous studies [5, 6, 17], which provided acceptable results with minimal computational cost. It

is well known that a large number of meshes requires more computational resources notably in terms of time, memory, and storage [18, 19]. A small-scale model minimizes the number of mesh elements, thus providing an efficient simulation process. Three different train exit positions were employed, and these are illustrated in Figure 1. These positions are identified as Cases A, B, and C, representing different scenarios of the train exiting the tunnel.

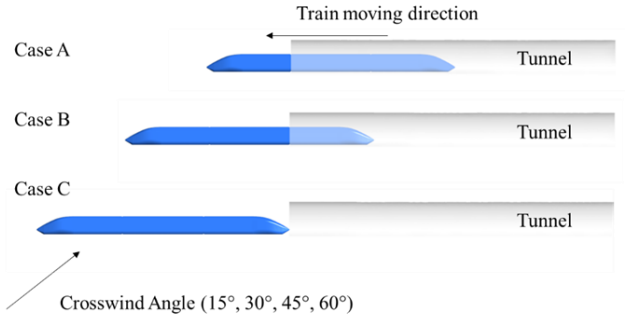

Figure 1 Illustrations of three tunnel exiting positions during crosswinds, denoted as Cases A, B, and C

For the current study, a simplified 3-D version of NG-HST was chosen which is developed by German Aerospace Centre (DLR). The train consists of three carriages, including a front carriage, a rear carriage, and a middle carriage [20]. The full-scale length of the rear or front carriage and middle carriage are approximately 21 m and 20 m, respectively [21]. The detailed dimensions of both the train model and tunnel can be found in Figure 2. The tunnel is designed (length, height, and width) based on a previous study using SolidWorks software [5].

2.2 Boundary Conditions

The virtual wind tunnel or computational domain for the simulation is separated into two parts for predicting the fluid flow: the open area for the train exit and the tunnel. To simulate crosswinds, a side wall of the enclosure was chosen as the crosswind inlet (velocity inlet) alongside the main inlet (velocity inlet). There were two outlets (as pressure outlets), one opposite the crosswind inlet and one at the tunnel's end. The floor was considered as the no-slip wall. Furthermore, the remaining walls are defined as wall boundaries. Figure 3 depicts the computational domain, including boundary conditions. The height of the train, denoted as *H*, serves as the characteristic length used for determining the Reynolds number in the context of the aerodynamics of the train, with a train speed of 111.11 m/s (approximately 400 km/h) [5] providing a Reynolds number, *Re* 1.3×10^6.

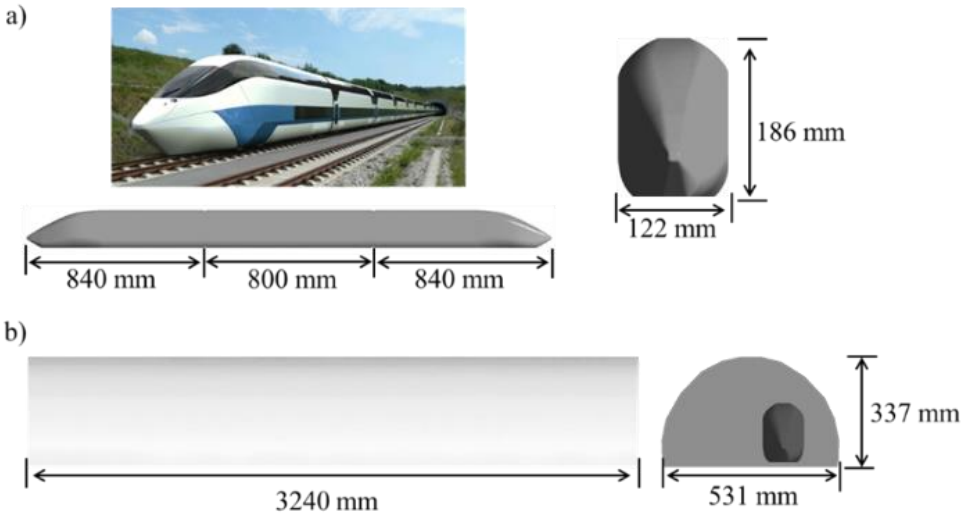

Figure 2 Detailed dimensions of a) the Next-Generation High-Speed Train (NG-HST) model, including the front carriage, middle carriage, and rear carriage, and b) the tunnel.

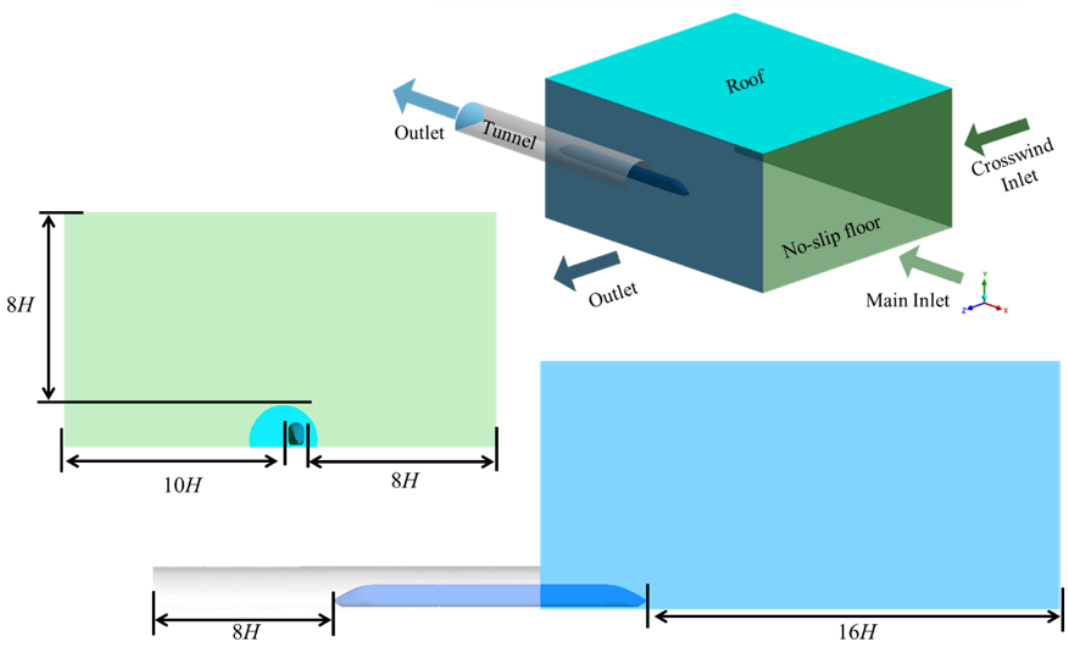

Figure 3 Details of the computational domain and its boundary conditions. The computational domain is meticulously depicted, showcasing the virtual wind tunnel utilized for the simulation

The size of the domain was made sufficiently large for the simulation. This allows to capture the fluid flow around the train at the exit of the tunnel. Furthermore, the left side of the train leaving region was 2*H* greater than the right side, as flow structure usually forms on the leeward side due to crosswinds. The distance between bottom surface of the train and the ground was 0.13*H*. Previous studies show that, crosswind velocity between 20-35 m/s significantly impacts the safety, stability, and aerodynamic performance of high-speed trains [22–24]. Thus, a constant wind velocity of 25 m/s was considered as the crosswind velocity [6, 25]. This study considered four crosswind angles: 15°, 30°, 45°, and 60° [26]. It has been reported that the effects of crosswind on train aerodynamics increase with crosswind angle and begin to decrease after 60° yaw angle [27, 28]. In this study, the maximum angle of attack was defined to be 60° yaw. Aside from that, both pressure outlets define atmospheric pressure.

2.3 Numerical Setup

ANSYS Fluent was used to solve the Navier-Strokes equations to predict the flow behavior around the train when exiting the tunnel. In this study, the SIMPLE algorithm was employed for pressure-velocity coupling since it leverages mass conservation to create pressure fields. This algorithm is relevant in this case due to its effectiveness in solving the fundamental governing equations of fluid mechanics, which is essential for complex flow phenomena and turbulence modeling of trains [29, 30]. Furthermore, during spatial discretization, the second order upwind was used for the pressure, momentum, turbulent kinetic energy, and turbulent dissipation rate. Meanwhile, Unsteady Reynolds-averaged Navier-Stokes (URANS) equations combined with the *k-ε* turbulence model were used to solve the fluid flow. The URANS method has been highlighted as a suitable approach for dealing with the Navier-Stokes equations, reducing computational complexity while ensuring accuracy [31].

2.4 Mesh Generation and Grid Independence Study

In the computation domain, a structured type mesh was used. It was discovered that structured meshes required lesser computational resources than unstructured meshes [32]. Furthermore, structured mesh is appropriate for this study because a simplified geometry is used. Ansys Advanced Meshing was used to create hexa-dominant meshes. By adjusting the meshing parameters outlined in Table 1, low, medium, and high quality meshes were generated to determine the optimal meshes for the simulation. Figure 4 depicts the details of the three mesh resolutions.

Table 1 Meshing parameters description for grid independence study

Parameter	Coarse	Medium	Fine
Mesh (max. el. Size)	256 mm	128 mm	64 mm
Face (size)	20 mm	10 mm	5 mm
Affected Diameter	2 mm	4 mm	8 mm
Elements Number	235482	392493	631925

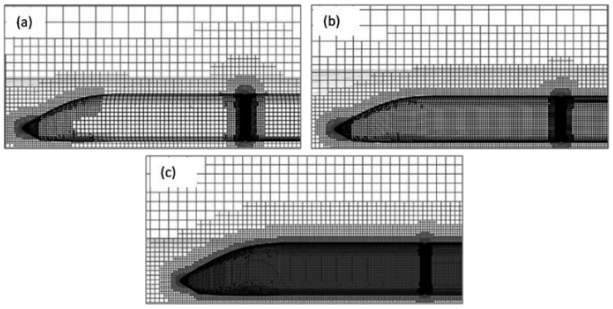

Figure 4 Meshing on the geometry depicting a) coarse mesh, b) medium mesh, and c) fine mesh configurations

Grid independence test (GIT) results where drag coefficient value was compared to previous study [33]. It should be noted that the GIT results were obtained using the front car and half of the middle car because wind tunnel data was only available for that. The results show that as the mesh gets finer, the drag coefficient value begins to converge as in Table 2. The drag coefficient for medium and fine meshes is the same as the experimental value. Which means that a medium mesh is sufficient to predict the coefficient of aerodynamic loads. Furthermore, running the final case simulations would be enough using a medium mesh. However, a finer mesh around the train is necessary to capture the flow structure. Thus, approximately 6 million meshes have been used during final simulations.

Table 2 Comparison of drag coefficient value with different mesh quality and previous study [33]

Result	Coarse	Medium	Fine	Exp. value
Drag coefficient	0.19	0.18	0.18	0.18

3.0 RESULTS AND DISCUSSION

This section discusses the vortex structure around the train when exiting a tunnel with crosswinds. A vortex is a mass of spinning fluid or air. Vortices are formed due to the interaction of fluids with different velocities, resulting in rotational flow structures [34]. As high-speed trains move through the air, vortices of varying strengths are rapidly generated and shed, particularly in the near wake area. These vortices not only increase pressure drag but also have a substantial impact on the lift and side forces of the trailing car [35]. The presence of streamwise vortices and the associated impingement of high-speed fluid on the train's surface is correlated with an increase in skin friction, further contributing to the overall drag experienced by the train [36].

Figure 5-7 represents the vortex core around the train at different positions of the tunnel exit under crosswinds. The vortices are coloured by pressure, and the results indicate that a complex and unsteady flow structure is formed on the leeward side of the train due to the crosswinds from the windward side. To investigate the effect of crosswind on the train, three cases were considered based on the carriage position at the tunnel exit: one car exit, two car exit, and three car exits. The black dashed arrows serve to illustrate vortices that are reflected by the tunnel wall and subsequently move downstream. In contrast, the red dashed arrow is used to highlight major vortices that pass through the train wall. This distinction in arrow representation aids in distinguishing the two types of vortex behaviors in the context of the flow dynamics.

Figure 5 shows the fluid flow formed around the train while only one car is exiting the tunnel under crosswind conditions. Theoretically, this complex and unsteady flow depends on the wind and weather conditions. At a yaw angle of 15°, major vortices, V_{nose} (red dotted region) formed at the lower and upper areas of the nose area [37]. A vortex is formed in a twister-like shape as the yaw angle increases to 60°. Even though at a lower yaw angle most of the vortices formed on the leeward side seem attached to the train surface, the situation changes at a higher yaw angle. So, it can be noticed that at 60° yaw angle, most of the vortices detach from the train body, except for some small eddies at both the lower and upper edges of the train. Meanwhile, pressure tends to be high on the windward side. This is also increasing as the yaw angle gets larger. In addition, peak pressure can be seen near the tunnel's exiting wall and extended to half of the middle car. A small part of the air flow entered the tunnel using the space between the tunnel wall and the train. A large part of the air passed downstream. Due to the blockage by the tunnel wall, the rest of the airflow entered the tunnel. This situation is said to improve as the wind angle increases. This also reflects that effects of the crosswind on aerodynamic loads can be severe as train surface respect to the wind direction is increased. If, in this situation, another train enters the tunnel from the opposite direction, flow on the leeward side may affect the aerodynamic performance of the train.

Flow around the train while two carriages exit the tunnel shown in Figure 6. When a high-speed train enters a tunnel, it generates pressure waves that propagate through the tunnel, causing complex pressure variations both inside the tunnel and on the surface of the train [38]. These pressure fluctuations are a result of the superposition of inlet pressure waves and air disturbances caused by the passing train [39]. A complex flow structure tends to be identified on the leeward side of the front carriage due to the pressure instability. Vortices were mostly formed at the bottom and upper edges of the middle car. Yet, no significant effect was visible in terms of flow structure while increasing crosswind angle. For all the crosswind angles, air flow entered the tunnel using the empty space between tunnel wall and the train on the windward side. Conversely, a large amount of the air flowed into the tunnel. For instance, at a 15° yaw angle, a vortex forms at the inter-car gap and moves towards the tunnel. In addition, two large vortices also

formed and were supposed to flow downstream; however, due to the tunnel wall, airflow was blocked and flowed inside the tunnel area. The figure also shows that pressure on the windward side is increased with a higher angle of crosswind. This phenomenon is also supported by a previous study. When a train enters a tunnel, the presence of the train wall and the tunnel wall restricts the air flow, causing the air in front of the train to be compressed and move forward along the tunnel axis, resulting in a sudden increase in pressure in front of the train [40].

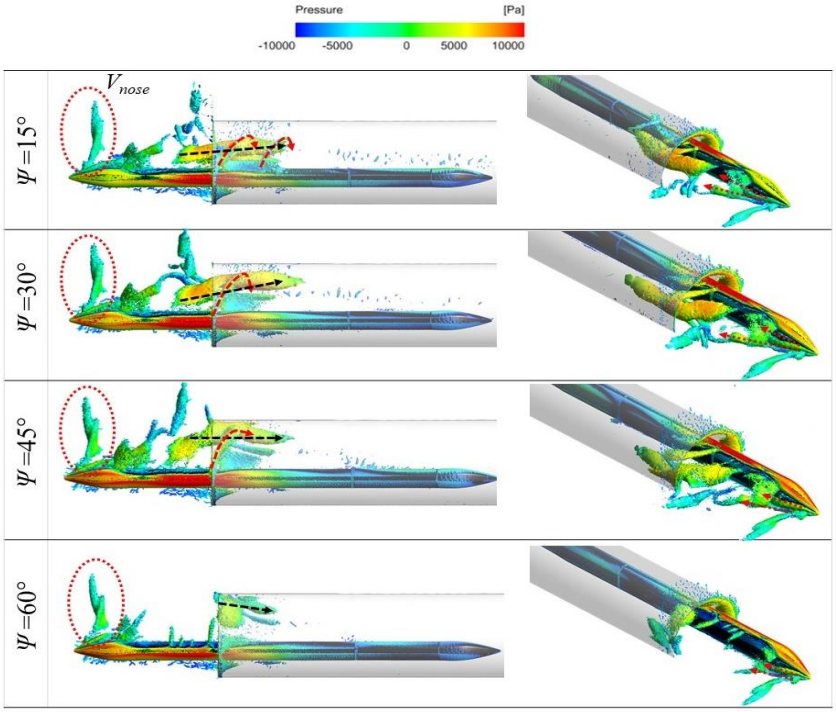

Figure 5 Visualization of the flow structure around the train for Case A, showing variations at different yaw angles

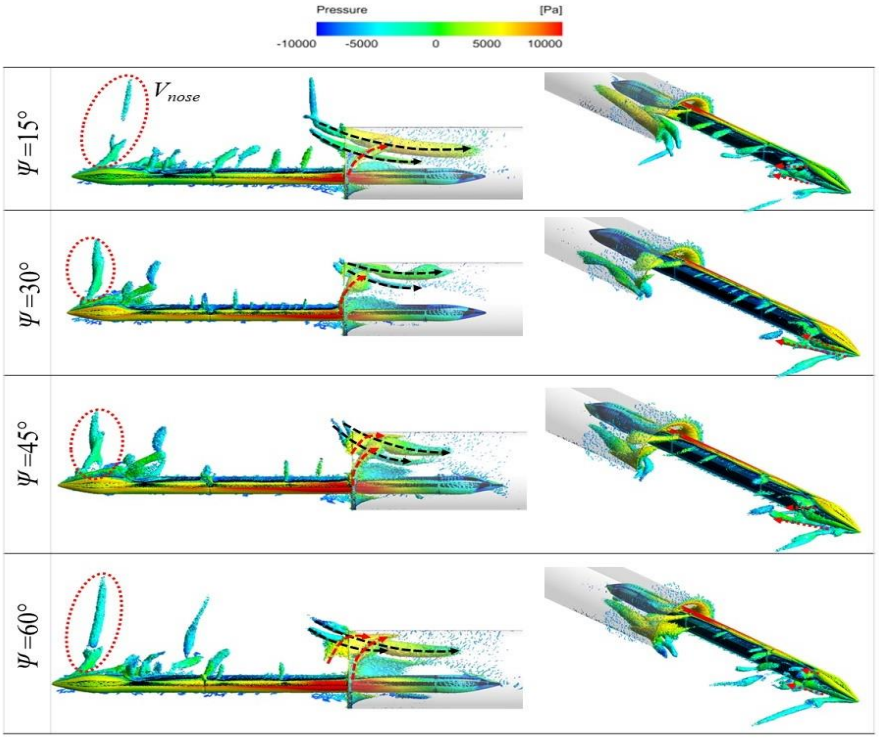

Figure 6 Illustration of the flow structure around the train for Case B, showing changes at different yaw angles

Figure 7 illustrates the vortex structure around the train as it escaped the tunnel during strong crosswinds. The flow structure on the train's leeward side began to experience less infrastructural effect as it exited the tunnel. Vortices were attached to the head car on the leeward side, and the distance between the vortex and the train increased as the train moved further. Furthermore, the angle between the vortex on the leeward side and the train increased, as did the yaw angle. The train's wake created a complex flow structure. Part of the wake vortices appear to have flowed downstream; however, the flow entered the tunnel due to a blocking effect caused by the tunnel wall. This situation results in a phenomenon in which the complex flow structure formed by the various angles of wind loads interacts with the train and tunnel [41]. Furthermore, studies have indicated that the flow on the sides of intermediate cars of a high-speed train contains vortical structures generated near the under-corners of those cars facing the tunnel wall, emphasizing the intricate nature of the flow around the train in tunnel environments [42]. As a result, the aerodynamic characteristics of the NG-HST exiting the tunnel are heavily influenced by this flow behavior.

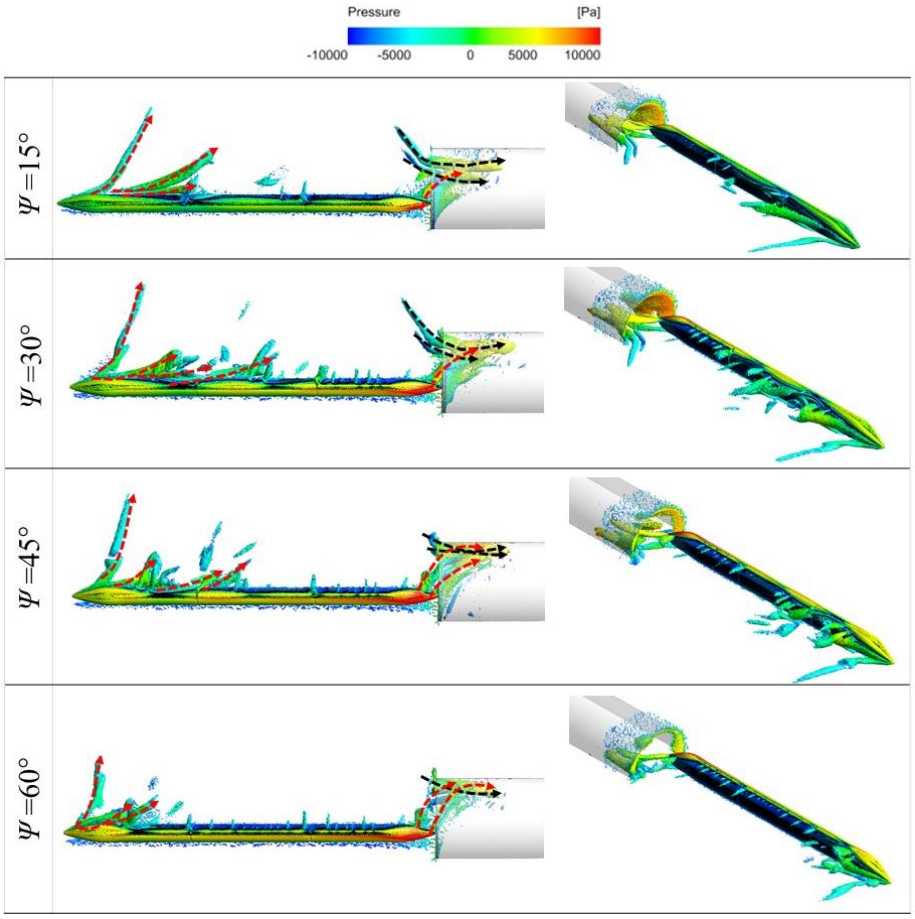

Figure 7 Flow structure around train for case C at different yaw angles

4.0 CONCLUSION

In this study, unsteady RANS was employed to investigate the flow behavior around the NG-HST model as it exited a tunnel under strong crosswind conditions, utilizing the k-ε turbulence model to predict turbulent flow around the train.

The CFD simulation results revealed that a significant portion of the airflow entered the tunnel during the train's exit under strong crosswind conditions, with notable changes observed as the yaw angle increased from 15° to 60°. For cases A and B, positive pressure on the leeward side was lower compared to the windward side, indicating a substantial impact of crosswind on the aerodynamic performance. The crosswind effects on the carriages outside the tunnel showed higher pressure compared to those inside the tunnel. As the train fully exited the tunnel, unsteady behavior became noticeable in the flow structure due to the crosswind effect, particularly around the head carriage, which is crucial for safe train operation. Therefore, safety measures should be considered for trains exiting tunnels in the presence of strong crosswinds.

It is important to note some limitations in our study and simulation approach. For instance, we specifically examined yaw angles from 15° to 60°, so applying our findings to different angles should be done carefully.

Additionally, we assumed steady-state conditions, and exploring transient behavior during train exits could be a worthwhile future investigation. Despite these limitations, our results provide useful insights for enhancing wind barriers and infrastructure along railways to improve the stability and safety of high-speed trains.

Acknowledgement

This research was financially supported by the Ministry of Higher Education, Malaysia through (FRGS/1/2022/TK02/UTHM/03/1).

Conflicts of Interest

The author(s) declare(s) that there is no conflict of interest regarding the publication of this paper.

References

[1] Liu, D., Marita Tomasini, G., Rocchi, D., Cheli, F., Lu, Z., and Zhong, M. 2020. Correlation of Car-body Vibration and Train Overturning under Strong Wind Conditions. *Mechanical Systems and Signal Processing*. 142: 106743. Doi: https://doi.org/10.1016/j.ymssp.2020.106743.

[2] Yang, W., Deng, E., Zhu, Z., He, X., and Wang, Y. 2020. Deterioration of Dynamic Response during High-speed train Travelling in Tunnel–bridge–tunnel Scenario under Crosswinds. *Tunnelling and Underground Space Technology*. 106: 103627. Doi: https://doi.org/10.1016/j.tust.2020.103627.

[3] Hoppmann, U., Koenig, S., Tielkes, T., and Matschke, G. 2002. A Short-term Strong Wind Prediction Model for Railway Application: Design and Verification. *Journal of Wind Engineering and Industrial Aerodynamics*. 90(10): 1127-1134. Doi: https://doi.org/10.1016/S0167-6105(02)00226-X.

[4] Rocchi, D., Tomasini, G., Schito, P., and Somaschini, C. 2018. Wind Effects Induced by High Speed Train Pass-by in Open Air. *Journal of Wind Engineering and Industrial Aerodynamics*. 173: 279-288. Doi: https://doi.org/10.1016/j.jweia.2017.10.020.

[5] Arafat, M. and Ishak, I. A. 2022. CFD Analysis of the Flow around Simplified Next-generation Train Subjected to Crosswinds at Low Yaw Angles. *CFD Letters*. 14(3): 129-139. Doi: https://doi.org/10.37934/cfdl.14.3.129139.

[6] Arafat, M. and Ishak, I. A. 2023. Aerodynamic Performance of a Next-generation High-speed Train under Transient Crosswind. Doi: https://doi.org/10.31219/osf.io/u3mqb.

[7] Tian, H, Huang, S., and Yang, M. 2015 Flow Structure around High-speed Train in Open Air. *Journal of Central South University*. 22(2): 747-752. Doi: https://doi.org/10.1007/s11771-015-2578-7.

[8] Guo, Z., Liu, T., Chen, Z., Liu, Z., Monzer, A., and Sheridan, J. 2020. Study of the Flow Around Railway Embankment of Different Heights with and without Trains. *Journal of Wind Engineering and Industrial Aerodynamics*. 202: 104203. Doi: https://doi.org/10.1016/j.jweia.2020.104203.

[9] Tomasini, G., Giappino, S., and Corradi, R. 2014. Experimental Investigation of the Effects of Embankment Scenario on Railway Vehicle Aerodynamic Coefficients. *Journal of Wind Engineering and Industrial Aerodynamics*. 131: 59-71. Doi: https://doi.org/10.1016/j.jweia.2014.05.004.

[10] Xue, F., Han, Y., Zou, Y., He, X., and Chen, S. 2020. Effects of Wind-barrier Parameters on Dynamic Responses of Wind-road Vehicle–bridge System. *Journal of Wind Engineering and Industrial Aerodynamics*, 206: 104367. Doi: https://doi.org/10.1016/j.jweia.2020.104367.

[11] He, X. H., Zou, Y. F., Wang, H. F., Han, Y., and Shi, K. 2014. Aerodynamic Characteristics of a Trailing Rail Vehicles on Viaduct based on Still Wind Tunnel Experiments. *Journal of Wind Engineering and Industrial Aerodynamics*. 135: 22-33. Doi: https://doi.org/10.1016/j.jweia.2014.10.004.

[12] Montenegro, P. A., Heleno, R., Carvalho, H., Calçada, R., and Baker, C. J. 2020. A Comparative Study on the Running Safety of Trains Subjected to Crosswinds Simulated with different wind models. *Journal of Wind Engineering and Industrial Aerodynamics*. 207: 104398. Doi: https://doi.org/10.1016/j.jweia.2020.104398.

[13] Yao, Z., Zhang, N., Chen, X., Zhang, C., Xia, H., and Li, X. 2020. The Effect of Moving Train on the Aerodynamic Performances of Train-bridge System with a Crosswind. *Engineering Applications of Computational Fluid Mechanics*. 14(1): 222-235. Doi: https://doi.org/10.1080/19942060.2019.1704886.

[14] Diedrichs, B., Sima, M., Orellano, A., and Tengstrand, H. 2007. Crosswind Stability of a High-speed Train on a high Embankment. *Proceedings of the Institution of Mechanical Engineers, Part F: Journal of Rail and Rapid Transit*. 221(2): 205-225. Doi: https://doi.org/10.1243/0954409JRRT126.

[15] Wang, L., Luo, J., Li, F., Guo, D., Gao, L., and Wang, D. 2021. Aerodynamic Performance and Flow Evolution of a High-speed Train Exiting a Tunnel with Crosswinds. *Journal of Wind Engineering and Industrial Aerodynamics*. 218: 104786. Doi: https://doi.org/10.1016/j.jweia.2021.104786.

[16] Yang, M. Z., Zhou, D., Zhang, J., and Zhou, W. Bin. 2010. Research on the Influence of Shaft Area on Alleviating Tunnel Aerodynamic Effects through Dynamic Model Test. *Proceedings - 2010 International Conference on Optoelectronics and Image Processing, ICOIP 2010*. 2: 305-309. Doi: https://doi.org/10.1109/ICOIP.2010.158.

[17] Arafat, M., Amin Ishak, I., Mohammad, A. F., Khalid, A., Mohmad Jaát, M. N., and Yasak, M. F. 2023. Effect of Reynolds Number on the Wake of a Next-Generation High-Speed Train using CFD analysis. *CFD Letters*. 15(1): 76-87. Doi: https://doi.org/10.37934/cfdl.15.1.7687.

[18] Imai, Y. and Aoki, T. 2006. A Higher-order Implicit IDO Scheme and Its CFD Application to local Mesh Refinement Method. *Computational Mechanics*. 38(3): 211-221. Doi: https://doi.org/10.1007/s00466-005-0742-x.

[19] Belloch, J. A., Amor-Martin, A., Garcia-Donoro, D., Martínez-Zaldívar, F. J., and Garcia-Castillo, L. E. 2019. On the Use of Many-core Machines for the Acceleration of a Mesh Truncation Technique for FEM. *Journal of Supercomputing*. 75(3): 1686-1696. Doi: https://doi.org/10.1007/s11227-018-02739-9.

[20] Zhang, L., Yang, M., and Liang, X. 2018. Experimental Study on the Effect of Wind Angles on Pressure Distribution of Train Streamlined Zone and Train Aerodynamic Forces. *Journal of Wind Engineering and Industrial Aerodynamics*. 174: 330-343. Doi: https://doi.org/10.1016/j.jweia.2018.01.024.

[21] Winter, J. 2012. Novel Rail Vehicle Concepts for a High Speed Train: The Next Generation Train. *Civil-Comp Proceedings*. Doi: https://doi.org/10.4203/ccp.98.22.

[22] Du, L., Bian, C., and Zhang, P. 2022 Influence of Structural Types of CRTS I Plate-Type Ballastless Track on Aerodynamic Characteristics of High-Speed Train. *Urban Rail Transit*. 8(3-4): 267-285. Doi: https://doi.org/10.1007/s40864-022-00173-y.

[23] Han, Y., Liu, Y., Hu, P., Cai, C. S., Xu, G., and Huang, J. 2020. Effect of Unsteady Aerodynamic Loads on Driving Safety and Comfort of Trains Running on Bridges. *Advances in*

Structural Engineering. 23(13): 2898-2910.
Doi: https://doi.org/10.1177/1369433220924794.
[24] Liang, H., Sun, Y., Li, T., and Zhang, J. 2023. Influence of Marshalling Length on Aerodynamic Characteristics of Urban Emus under Crosswind. *Journal of Applied Fluid Mechanics*. 16(1): 9-20.
Doi: https://doi.org/10.47176/jafm.16.01.1338.
[25] Sun, Z., Hashmi, S. A., Dai, H., and Li, G. 2022. Safety of a High-speed Train Passing by a Windbreak Breach under Different Wind Speeds. *Proceedings of the Institution of Mechanical Engineers, Part F: Journal of Rail and Rapid Transit*. 236(8): 899-906.
Doi: https://doi.org/10.1177/09544097211046095.
[26] Huo, X., Liu, T., Yu, M., Chen, Z., Guo, Z., Li, W., and Wang, T. 2021. Impact of the Trailing Edge Shape of a Downstream Dummy Vehicle on Train Aerodynamics Subjected to Crosswind. *Proceedings of the Institution of Mechanical Engineers, Part F: Journal of Rail and Rapid Transit*. 35(2): 201-214.
Doi: https://doi.org/10.1177/0954409720915039.
[27] Baker, C. J., Jones, J., Lopez-Calleja, F., and Munday, J. 2004. Measurements of the Cross Wind Forces on Trains. *Journal of Wind Engineering and Industrial Aerodynamics*. 92(7-8): 547-563.
Doi: https://doi.org/10.1016/j.jweia.2004.03.002.
[28] Cheli, F., Ripamonti, F., Rocchi, D., and Tomasini, G. 2010. Aerodynamic Behaviour Investigation of the New EMUV250 Train to Cross Wind. *Journal of Wind Engineering and Industrial Aerodynamics*. 98(4-5): 189-201.
Doi: https://doi.org/10.1016/j.jweia.2009.10.015.
[29] Klein, B., Müller, B., Kummer, F., and Oberlack, M. 2016. A High-order Discontinuous Galerkin Solver for Low Mach Number Flows. *International Journal for Numerical Methods in Fluids*. 81(8): 489-520.
Doi: https://doi.org/10.1002/fld.4193.
[30] Khawaja, H. and Moatamedi, M. 2018. Semi-implicit Method for Pressure-linked Equations (SIMPLE) ⇓ Solution in MATLAB®. *International Journal of Multiphysics*. 12(4): 313-325.
Doi: https://doi.org/10.21152/1750-9548.12.4.313.
[31] Zhou, D., Li, J., Hu, T., and Chen, T. 2023. Influence of Subway Train Fire Locations on the Characteristics of Smoke Movement in a Curved Tunnel. *PLoS ONE*. 18(1 January).
Doi: https://doi.org/10.1371/journal.pone.0279818.
[32] Bern, M. and Plassmann, P. 2000. Mesh Generation. In: J.-R. Sack, J. Urrutia, (Eds.), *Handbook of Computational Geometry* (291-332). Elsevier.
Doi: https://doi.org/10.1016/b978-044482537-7/50007-3
[33] Fragner, M. M., Weinman, K. A., Deiterding, R., Fey, U., and Wagner, C. 2015. Comparison of Industrial and Scientific CFD Approaches for predicting Cross Wind Stability of the NGT2 Model Train Geometry. *International Journal of Railway Technology*. 4(1): 1-28.
Doi: https://doi.org/10.4203/ijrt.4.1.1.
[34] Nakamura, Y., Nakashima, T., Shimizu, K., Hiraoka, T., Nouzawa, T., Kanehira, T., and Mutsuda, H. 2023. Identification of Wake Vortices using a Simplified Automobile Model under Parallel Running and Crosswind Conditions. *Journal of Fluid Science and Technology*. 18(1).
Doi: https://doi.org/10.1299/JFST.2023JFST0005.
[35] Liu, W., Guo, D., Zhang, Z., Chen, D., and Yang, G. 2019. Effects of Bogies on the Wake Flow of a High-Speed Train. *Applied Sciences*. 9(4): 759.
Doi: https://doi.org/10.3390/app9040759.
[36] Hammond, E. P., Bewley, T. R., and Moin, P. 1998. Observed Mechanisms for Turbulence Attenuation and Enhancement in Opposition-controlled Wall-bounded Flows. *Physics of Fluids*. 10(9): 2421-2423.
Doi: https://doi.org/10.1063/1.869759.
[37] LI, R. and MEI, Y. 2017. Study on the Aerodynamic Performance of the High-Speed Train Head with Symmetrical and Asymmetric Nose Shape. *DEStech Transactions on Engineering and Technology Research*.
Doi: https://doi.org/10.12783/dtetr/icia2017/15687
[38] Kim, J. H. and Rho, J. H. 2018. Pressure Wave Characteristics of a High-speed Train in a Tunnel According to the Operating Conditions. *Proceedings of the Institution of Mechanical Engineers, Part F: Journal of Rail and Rapid Transit*. 232(3): 928-935.
Doi: https://doi.org/10.1177/0954409717702015.
[39] Wang, X. Y. 2018. Numerical Analysis on Aerodynamic Behavior of High-speed Trains in the Tunnel and Open Air based on the Virtual Reality Technology. *Journal of Vibroengineering*. 20(2): 1144-1160.
Doi: https://doi.org/10.21595/jve.2017.18430.
[40] Lu, Y., Zhang, D., Zheng, H., Lu, C., Chen, T., Zeng, J., and Wu, P. 2019. Analysis of the Aerodynamic Pressure Effect on the Fatigue Strength of the Carbody of High-speed Trains Passing by Each Other in a Tunnel. *Proceedings of the Institution of Mechanical Engineers, Part F: Journal of Rail and Rapid Transit*. 233(8): 783-801.
Doi: https://doi.org/10.1177/0954409718809469
[41] Miao, X., He, K., Minelli, G., Zhang, J., Gao, G., Wei, H., He, M., and Krajnovic, S. 2020. Aerodynamic Performance of a High-Speed Train Passing through Three Standard Tunnel Junctions under Crosswinds. *Applied Sciences*. 10(11): 3664.
Doi: https://doi.org/10.3390/app10113664.
[42] Sakuma, Y., Païdoussis, M. P., and Price, S. J. 2008. Dynamics of Trains and Train-like Articulated Systems Travelling in Confined Fluid—Part 2: Wave Propagation and Flow-excited Vibration. *Journal of Fluids and Structures*. 24(7): 954-976.
Doi: https://doi.org/10.1016/j.jfluidstructs.2008.01.003.